




# Aberrant brain structural network and altered topological organization in minimal hepatic encephalopathy

Lu-Bin Gou\*   
Wei Zhang\*   
Da-Jing Guo   
Wei-Jia Zhong   
Xiao-Jia Wu   
Zhi-Ming Zhou 

## PURPOSE

We aimed to investigate the multilevel impairments of brain structural network in patients with minimal hepatic encephalopathy (MHE).

## METHODS

Twenty-two patients with MHE and 22 well-matched healthy controls (HC) underwent structural magnetic resonance imaging (MRI) brain scans and neuropsychological evaluations. Individual brain structural networks were constructed using diffusion tensor imaging. Comparing with HC, we investigated the possible impairments of brain structural network in MHE, by applying graph-theory approaches to analyze the topological organization at global, modular, and local levels. The correlations between altered brain structural network and neuropsychological tests scores and venous ammonia levels were also examined in MHE patients.

## RESULTS

In the MHE group, small-worldness showed significant decrease and normalized characteristic path length showed increase at the global level. In the modular section, six modules were identified. The inter-modular connective strengths showed significant increase between modules 2 and 4 and between modules 4 and 5. The results of node analysis showed similar hub distributions in the MHE and HC groups except for the right postcentral gyrus, which was only found in the MHE group. No significant differences were found in connective strength of edges between MHE and HC groups using network-based statistics.

## CONCLUSION

The altered brain structural networks with reduced network integration and module segregation were demonstrated in patients with MHE. The dysconnectivity of brain structural network could provide an explanation for the brain dysfunctions of MHE.

Minimal hepatic encephalopathy (MHE), characterized by the presence of mild cognitive impairments, executive dysfunction, attention disorder, and interference inhibition, is considered the initial phase in the spectrum of hepatic encephalopathy (HE), with an estimated prevalence of 30%–84% among patients with cirrhosis (1, 2). Due to its subtle clinical symptoms, the current diagnosis of MHE is only possible through specialized psychometric and neurophysiological measures. Notably, the mild neuropsychological and neurophysiological alterations reduce the patient's health-related quality of life (3, 4). More importantly, MHE tends to develop overt HE, which is associated with poor outcome (5). Therefore, a better understanding of the pathophysiologic mechanisms underlying these brain dysfunctions in MHE could lead to new biomarkers for selecting therapeutic strategies and evaluating prognosis in clinical trials.

New emerging brain network analyses provide insight into the basic neural substrates of neurologic diseases objectively. The human brain can be conceptualized as a complex network comprising functional associations or anatomical tracts among brain regions (6, 7), named as the brain functional network or the brain structural network. Graph theory, known as the approach of complex network analysis, promises to reliably quantify brain networks with neurobiologically meaningful topological measurements at global, modular, and local levels (8). Several resting state functional magnetic resonance imaging (MRI) stud-

From the Department of Radiology (L.B.G.), First Hospital of Lan Zhou University, Gansu, China; Department of Radiology (W.Z., D.J.G., W.J.Z., X.J.W., Z.M.Z. ✉ [zhouzhiming1127@163.com](mailto:zhouzhiming1127@163.com)), The Second Affiliated Hospital of Chongqing Medical University, Chongqing, China.

\*Lu-Bin Gou and Wei Zhang contributed equally to this work.

Received 20 April 2019; revision requested 16 August 2019; last revision received 18 September 2019; accepted 20 October 2019.

Published online 18 March 2020.

DOI 10.5152/dir.2019.19216

You may cite this article as: Gou LB, Zhang W, Guo DJ, Zhong WJ, Wu XJ, Zhou ZM. Aberrant brain structural network and altered topological organization in minimal hepatic encephalopathy. *Diagn Interv Radiol* 2020; 26:255–261.

ies have focused on the brain functional network of patients with MHE. The converging evidence suggests that individuals with MHE show altered small-world organization (9) and decreased connective strength in some intrinsic sub-networks (10–12), including default mode network, executive control network, and salience network.

Although these studies have greatly advanced our understanding about functional changes of the brain in MHE, it is notable that brain functional network is highly constrained by the brain structural network, since the white matter (WM) is the structural basis of brain information transfer (13). In addition, the brain functional network shows scan time dependence and functional association, which may fluctuate over time (13). Taken together, such evidence suggests that it is necessary to explore the alterations in the topological properties of the WM structural network to fully understand the underlying neuropathological mechanism in MHE. Previous studies suggested that widespread alterations in structural connections can be found in association with cognitive dysfunction in various neurologic diseases, such as hypertension (14) and Parkinson disease (15). One recent study showed that a progressively decreased trend for topological properties of brain structural network were found from healthy controls (HCs) to prior overt HE and some altered topological metrics were correlated with cognitive impairments (16). However, no studies have been performed to assess the brain structural network in patients with MHE. Currently, it is unknown whether such similar changes could be found in MHE and how impaired structural connectivity associates with clinical features.

In this study, we aimed to look for possible impairments of brain structural network in patients with MHE as suggested by applying graph-theory approaches to analyze

the topological organization compared with HCs. Additionally, the relationships between brain structural network alterations and cognitive performance and venous ammonia levels were also examined in patients with MHE.

## Methods

### Subjects

This study was approved by the Institutional Ethics Committee of our hospital (decision number No. (2018) 043) and all participants signed informed consents. Twenty-two nonalcoholic liver cirrhosis patients with MHE were recruited in our study from 2018 to 2019. For each patient, blood samples including venous ammonia, albumin, aspartate aminotransferase, alanine aminotransferase, total bilirubin, and prothrombin time were acquired within the first 24 hours in the hospital. Brain MRI evaluation and neuropsychological assessment including the number connection test A (NCT-A) and digit-symbol test (DST) were performed within 5 days after the diagnosis was made. First, nonalcoholic cirrhosis was diagnosed by two senior infectious disease physicians (Zeng WQ and Ling N) on the basis of symptoms, signs, imaging and biochemical examinations. The Child-Pugh score was calculated based on clinical and laboratory measurements for each patient. MHE was diagnosed if a liver cirrhosis patient showed two abnormal neuropsychological tests without clinically overt symptoms, according to the final report of the working party of 11th World Congress of Gastroenterology in Vienna in 1998 (17). The abnormal neuropsychological tests were defined as exceeding the reference value (based on the normal value of 120 healthy Chinese volunteers) by two standard deviations (18). Exclusion criteria were age  $\leq 18$  years or  $\geq 75$  years; left-handedness; inability to complete neurological scale test; MRI contraindications; head motion  $>1.0$  mm in translation or  $1.0^\circ$  in rotation during the MRI; any neurological/psychiatric diseases or drugs abuse.

Twenty-two age-, gender-, education-matched, and right-handed HCs were enrolled through advertising within the hospital and nearby communities. None of the HCs had any liver or neurological or psychiatric diseases. All HCs underwent the same brain MRI evaluation and neuropsychological assessment. No laboratory tests were performed in HCs.

### MRI data acquisition

MRI was performed using a 3.0 T scanner (Achieva, Philips Medical System) with an 8-channel sense coil, keeping eyes closed and head motionless during examination in all subjects. In addition, the subjects were given earplugs and fixed with sponges of different thicknesses. MRI datum included conventional sequences (axial T1-weighted imaging, T2-weighted imaging, T2-weighted fluid-attenuated inversion recovery imaging and sagittal T1-weighted imaging), three-dimensional T1-weighted imaging, and diffusion tensor imaging (DTI). Three-dimensional T1-weighted images were acquired in the sagittal plane using a fast-field echo sequence (repetition time [TR], 7.4 ms; echo time [TE], 3.6 ms; flip angle,  $8^\circ$ ; FOV,  $250 \times 250$  mm<sup>2</sup>; matrix,  $228 \times 227$ ; slice number, 150; slice thickness, 1.1 mm with no gap; voxel size,  $1.1 \times 1.1 \times 1.1$  mm<sup>3</sup>). The DTI images were acquired covering the whole brain using a spin echo-based echo planar imaging sequence in the axial plane, including 15 volumes with diffusion gradients applied along 15 independent orientations with  $b$  value 800 s/mm<sup>2</sup> after the volume of  $b$  value 0 s/mm<sup>2</sup>. The scanning parameters of DTI sequence were as follows: TR, 6973 ms; TE, 75 ms; flip angle,  $90^\circ$ ; FOV,  $224 \times 224$  mm<sup>2</sup>; matrix,  $112 \times 112$ ; slice number, 65; voxel size,  $2 \times 2 \times 2$  mm<sup>3</sup>).

### DTI preprocessing and tractography

All DTI images preprocessing and network construction were implemented in a manner similar to our previous study (19) by using a pipeline toolbox, Diffusion Connectome Pipeline (DCP, <https://www.nitrc.org/projects/dcp>), which is a toolbox of MATLAB 2017a (MathWorks). First, stripping non-brain tissue and estimating the brain mask were performed. Second, the eddy-current effect and simple head-motion were corrected. Then, the diffusion tensor and fraction anisotropy matrix were calculated on a voxel-wise. Finally, whole-brain WM fibers reconstruction was performed. Deterministic tractography used the Fiber Assignment by Continuous Tracking (FACT) algorithm and terminated if a voxel with fraction anisotropy of less than 0.2 or encountering an angle of more than  $45^\circ$ .

### Network construction

Nodes and edges definition: Using the automated anatomical labeling (AAL) atlas, the cortical and subcortical regions (without cerebellum) were segmented as

#### Main points

- Small-worldness showed significant decrease at the global level in minimal hepatic encephalopathy (MHE).
- Normalized characteristic path length showed significant increase in MHE.
- The inter-module connectivity strength showed increase among some modules.
- A hub of right postcentral gyrus was identified in the MHE group but not in healthy controls.

90 nodes. The edges were represented by the WM tracts obtained by deterministic tractography linking each pair of nodes. We used the number of fibers as a measure of the strength of structural connectivity, namely the weight of edge.

**Network construction:** To ensure the accuracy of brain parcellation, we reoriented structural images to the Montreal Neurological Institution (MNI) template manually through Statistical Parametric Mapping 12 (SPM12, <http://www.fil.ion.ucl.ac.uk/spm/>). We used the DCP to obtain connectivity matrix (network) from the defined regions of interest (ROIs) and tractography for network construction. To avoid the presence of spurious fibers, we set all connections with the number of fibers fewer than three to zero. Individual brain structural network was constructed for each subject included in the study.

## Network analysis

### Topological properties of whole network

Graph theory was applied to analyze the topological properties of the brain structural network at global, modular, and local levels (20). At the global level, we explored global efficiency and characteristic path length to investigate the integration of the whole network. Segregation of the whole network was assessed by the clustering coefficient and local efficiency. The degree of small-world organization was assessed by the normalized characteristic path length, the normalized clustering coefficient, and small-worldness.

### Topological organization and properties of modules

A module is a group of densely interconnected nodes, which are often the basis for specialized submits of information processing, with a maximally possible number of intra-group links, and a minimally possible number of inter-group links in the brain structural network (20). At the modular level, we detected the component of modules using the optimization algorithms based on the mean network of all participants which were generated by the mean of the subject-specific networks and selected all connections that were present in more than 60% of all participants (21).

The intra-module and inter-module connectivity strength, as the basic topological properties of module, can be used to estimate the modular segregation (20). The in-

creased segregation is always with stronger intra-module and/or weaker inter-module connectivity strength, while the reduced segregation is with weaker intra-module and/or stronger inter-module connectivity strength. Furthermore, another primary measure of modular segregation is the participation coefficient, which quantifies the diversity of a brain node's connections across modules (20). Nodes with higher participation coefficient have connections with more modules. Conversely, nodes with low participation coefficient have connections with fewer modules.

### Topological properties of nodes and hubs identification

The local topological properties (degree centrality, betweenness centrality and eigenvector centrality) are obtained to assess the centrality or the importance of a node. In the brain structural network, hubs defined as nodes that are more important than other nodes, can interact with many other regions and play a key role in resilience to insults (22). However, only one single measure is not necessary and sufficient for assessing the importance and identifying hubs. The combination of three centralities provides a more robust method for hubs' detection. Hence, we employed the degree centrality, betweenness centrality and eigenvector centrality together to identify hubs regions, referring to a previous study (23). First, we calculated a group-averaged brain structural network for each group in which the weight of an edge was the mean of the weights across subjects and selected all connections that were present in more than 60% of group participants. Next, we calculated the three centralities and sorted them in descending order (from highest to lowest). The hubs of averaged WM-network were identified by determining whether a node belonged to: 1) the top 20% nodes with the highest level of degree centrality; 2) the top 20% nodes with the highest level of betweenness centrality; and 3) the top 20% nodes with the highest level of eigenvector centrality. If a node fulfilled the above three criteria, it was marked as a hub.

### Network based statistics

To detect the abnormal subnetworks with the altered connective strength of edges in brain structural network of MHE, we used a network-based statistic (NBS) approach, as in the methodology given by Zalesky et al.

(22). Briefly, we tested the defined hypothesis at every connection in the network independently. Then, chose a primary cluster-defining threshold to identify supra-threshold connections, within which the number of edges in subnetworks was then determined. Finally, a corrected *P* value was calculated for each subnetwork using the null distribution of maximal connected component size, which was derived empirically using a non-parametric permutation approach.

### Statistical analysis

To calculate significant differences of demographic and clinical characteristics, two independent-samples t-test was used to compare age, education years, NCT-A time, DST scores and venous ammonia levels between the MHE and HC groups.  $\chi^2$  test was used to analyze sex between the two groups. Analysis of covariance (ANCOVA) was applied to examine the difference in topological properties of network, module and node between the MHE and HC groups. The age and education years were set as covariates. For the comparisons of participant coefficient of 90 nodes, there was a multiple comparison problem. Therefore, we used the Bonferroni method to correct multiple comparison problem. In NBS, general linear models were used to examine the difference in connective strength (defined by FN) between the MHE and HC groups. The NBS corrected *P* value was calculated for each subnetwork using the null distribution of maximal connected component size, which was derived empirically using a nonparametric permutation approach (10 000 permutations). The range of primary test statistic threshold was set as 1 to 3 (interval 0.1). In order to examine whether symptoms severity (measured via NCT-A time and DST scores) and venous ammonia levels were associated with alterations in brain structural network, spearman correlation coefficients were calculated between the topological properties of network and module, and clinical and laboratory measurements in the MHE group. *P* < 0.05 was considered statistically significant.

## Results

The demographic and clinical characteristics of the subjects were summarized in Table 1. There were no significant differences in terms of age, gender, and years of education between the MHE and HC groups. Patients with MHE had significantly poorer neurocog-

Variables	MHE (n=22)	HC (n=22)	t	P
M/F ratio	16/6	14/8		0.517
Age (years)	57.82±10.08	56.27±10.03	0.510	0.810
Education (years)	9.68±3.06	10.77±4.15	-0.992	0.327
NCT-A (seconds)	73.18±22.53	34.68±13.42	6.885	0.000
DST (raw score)	18.86±6.74	46.54±13.03	-8.902	0.000
Venous ammonia (μmol/L)	12.77±7.34			
Child-Pugh (A/B/C)	11/7/4			

MHE, minimal hepatic encephalopathy; HC, healthy controls; M/F, male/female; NCT-A, number connection test A; DST, digit symbol test.

Global topological properties	MHE (n=22)	HC (n=22)	P
	Mean±SD	Mean±SD	
Global efficiency	18.50±3.252	18.69±2.095	0.871
Characteristic path length	0.06±0.11	0.05±0.006	0.582
Local efficiency	29.30±4.899	29.03±3.479	0.850
Clustering coefficient	0.04±0.007	0.04±0.008	0.484
Normalized clustering coefficient	3.48±0.329	3.60±0.349	0.211
Normalized characteristic path length	1.17±0.037	1.13±0.035	0.005
Small-worldness	2.99±0.307	3.17±0.271	0.033

MHE, minimal hepatic encephalopathy; HC, healthy controls; SD, standard deviation.

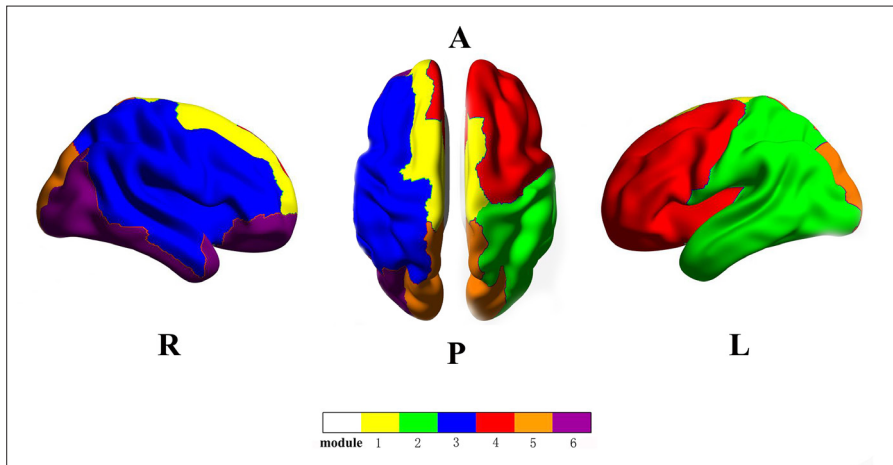


**Figure 1.** Six modules displayed in different colors are identified in the mean network of all participants. Anterior (A), posterior (P), left (L), and right (R).

nitive performance compared with HCs. In particular, patients with MHE showed longer time in NCT-A test and lower scores in DST test compared with the HC group.

At the global level, small-worldness showed significant decrease and normalized characteristic path length showed significant increase in the MHE group compared with the HC group. No significant differences were found in global efficiency,

characteristic path length, local efficiency, clustering coefficient and normalized clustering coefficient between the MHE and HC groups (Table 2).

Six modules were identified in the mean network of whole participants including module 1 (7 nodes), module 2 (20 nodes), module 3 (15 nodes), module 4 (19 nodes), module 5 (10 nodes) and module 6 (19 nodes) (Fig. 1). The inter-modular connective

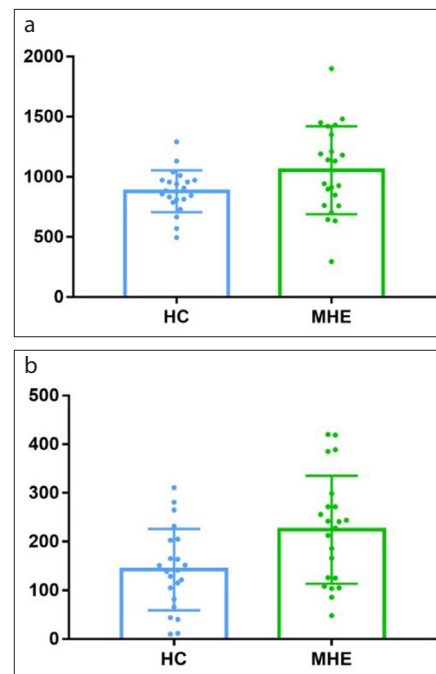


**Figure 2. a, b.** The inter-modular connective strengths show significant increase between module 2 and module 4 (a) and between module 4 and module 5 (b) in MHE group compared with HC group.

ive strengths showed significant increase between modules 2 and 4 (Fig. 2a) and between modules 4 and 5 (Fig. 2b) in the MHE group compared with the HC group. The results showed no significant differences of intra-modular connective strengths between the MHE and HC groups. There were no statistically significant changes in the participant coefficients of any nodes between the MHE and HC groups.

No significant differences were found in the topological properties of nodes between the MHE and HC groups.

There were 12 hubs found in the MHE group and 13 hubs found in the HC group. As shown in Fig. 3, the hubs organization of MHE patients was similar with HCs and eleven hubs (right precentral, bilateral superior frontal, bilateral middle frontal regions, left anterior cingulum, right middle cingulum, bilateral precuneus gyrus and bilateral putamen) were in both groups. One brain region (right postcentral gyrus) was identified as a hub in the MHE group but not in the HC group. Two brain regions (left middle occipital and right superior parietal gyrus) were identified as a hub in the HC group but not in the MHE group.

Compared with the HC group, no sub-networks with significantly reduced or increased connective strength were detected

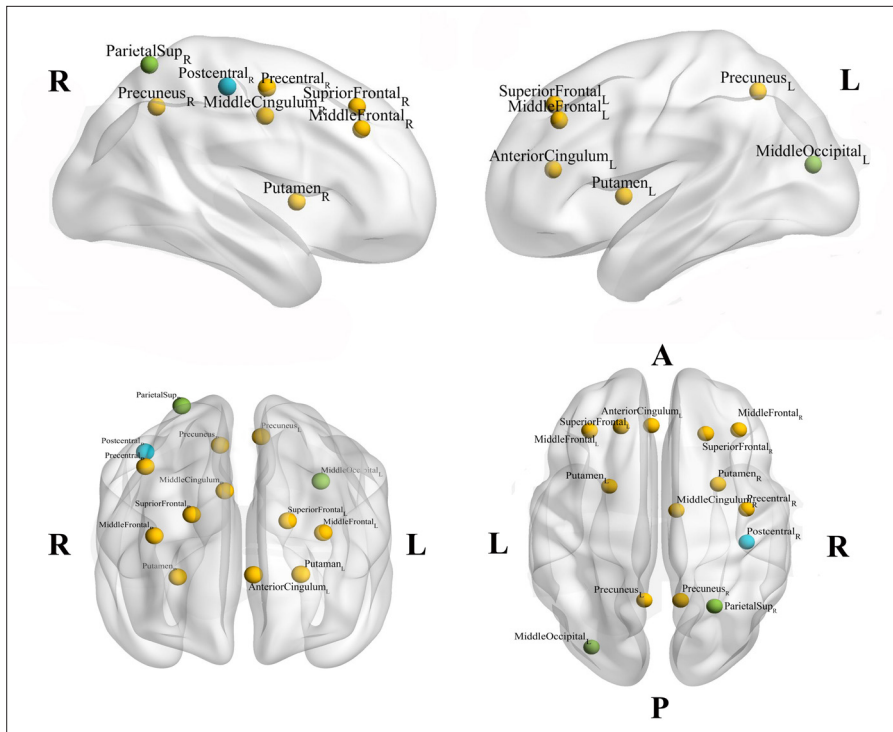


**Figure 3.** The hubs that are found in both MHE and HC groups are indicated by *yellow nodes*; the hub that is found only in MHE group is indicated by a *blue node*; and the hubs that are found only in HCs are indicated by *green nodes*. Anterior (A), posterior (P), left (L), and right (R).

at each primary test statistic threshold in the MHE group ( $P > 0.05$ , NBS corrected).

In the MHE group, the inter-module connective strength between modules 4 and 5 was negatively correlated with NCT-A time ( $r = -0.447$ ,  $P < 0.05$ ) and with venous ammonia levels ( $r = -0.426$ ,  $P < 0.05$ ), respectively. No significant correlations were found in the inter-module connective strength between modules 2 and 4. For the global topological properties, small-worldness, normalized and characteristic path length, no associations with NCT-A time, DST scores and venous ammonia levels were found in the MHE group.

## Discussion

Using brain structural network constructed by DTI and graph theory analysis, we investigated the altered structural brain connectome in nonalcoholic liver cirrhosis patients with MHE, for the first time. The main findings of our study were as follows: The MHE patients showed reduced information processing of the brain structural network, characterized by significantly decreased small-worldness and increased normalized characteristic path length. In the MHE group, the inter-module connectivity strength increased among modules,

which were mainly distributed in the left prefrontal, parietal, temporal and bilateral occipital regions. The left postcentral gyrus was the only node that belonged to the hubs of MHE patients rather than HCs.

The small-world architecture, which is an optimal balance between integration and segregation for fast and efficient information processing, has been proven in human brain network. Brain networks with higher small-worldness can integrate information from different modules at global level with faster speed as well as process information in segregated modules for the specific function in shorter time (24–26). A previous study about brain functional network showed that the small-worldness of functional brain network might be negatively correlated with the progression of MHE (27). Consistent with this study, our results showed that the degree of small-world organization of brain structural network was reduced in the MHE group. Especially, the reduction of small-worldness was mainly caused by the increase of normalized characteristic path length (the measurement of the capacity of network integration). Accordingly, our study indicated that the information integration within the whole brain was reduced in MHE patients. In ad-

dition, our results of the NCT-A and DST tests showed increased reaction time and slow processing speed in the MHE group, which was related to delayed information processing (one of the most common manifestations of MHE) (28). Therefore, impaired integration of brain structural network possibly explained the delay of information processing in MHE patients. Moreover, using an approach very similar to ours, Chen et al. (16) revealed that both integration and segregation of brain structural network show decrease in prior overt HE (the later stage of HE). Above all, these imaging evidences showed a progressively increased trend of the brain structural network deficit from MHE to HE. It also suggested the importance of early intervention on MHE.

The module is the basis of segregated information process, and the topological properties of module, which simply reflect the average segregation of the whole network, can estimate the altered segregation more precisely than global topological properties (20). Generally, the increased inter-modular connective strengths reflected the reduction of segregation between modules. In our study, we detected 6 modules. The inter-modular connective strengths of module 4 with module 2 and with module 5 showed increase in the MHE group compared with the HC group. The module 4 in our results mainly contained left prefrontal regions. It has been proven that prefrontal regions play an important role in the neuroanatomic basis of executive function (29). And the modules 2 and 5 in our study were both correlated with sensory information processing. In particular, module 2 mainly contained left parietal and temporal regions, while module 5 mainly included bilateral occipital regions. The temporal lobe is involved in processing auditory sensory. The occipital lobe is the visual information processing center, containing most of the anatomical region of the visual cortex. In addition, the parietal lobe integrates sensory information from various modalities, such as auditory and visual information (30).

Furthermore, the abnormalities of neuropsychological tests in our study reflected that the executive functions were impaired in patients with MHE. One important part of the executive function is the inhibitory control, which is a cognitive process that inhibits the dominant behavioral responses to outside stimuli in order to select a more ap-

appropriate behavior consistent with completing goals (31). In our study, the segregation between modules related with executive function and modules related with auditory and visual processing were reduced in MHE patients, and the information exchange across these regions increased as a consequence. Thus, the potential mechanism of executive dysfunction in patients with MHE may be that the auditory and visual stimuli are stronger in MHE patients than in HC so that the response to these stimuli cannot be inhibited sufficiently during executive behavior. With these interferences, the MHE patients cannot focus on completing goals. Similarly, previous study in adolescents also reported that the improved modular segregation of brain structural network supported the development of executive function (32). Altogether, our findings indicate that the impaired modular segregation may be mainly responsible for the impairment of inhibitory control and worsen the executive dysfunction in MHE patients.

Although there were no significant changes of node and edge in patients with MHE compared with HC in our study, alterations in hub distributions were identified in the MHE group. The right postcentral gyrus was found as a hub node only in the MHE group. It has been suggested that the hubs are valuable for integrative information processing and adaptive behavior (33, 34), but the hubs have also shown long connection distance, namely high wiring cost (35). Based on these theories, it has been suggested that the brain disorders were likely to impact preferentially on the hubs (36, 37). Therefore, the adjustment of hubs in our study indicated that the postcentral gyrus was vulnerable in the development of MHE. In other words, we can infer that postcentral gyrus would be affected when MHE progresses to HE. Our inference is in agreement with previous research, in which nodal efficiency of postcentral gyrus was found significantly abnormal in HE patients' functional network (38). The abnormality of postcentral cortical area was found to be implicated in lack of awareness and shortened attention (39), the onset of symptoms in grade 1 HE patients (40). Hence, the postcentral gyrus, the only altered hub in the MHE group, plays an important role in the disease progression of MHE.

Some limitations of our study should be noted. First, the sample size of both groups (MHE and HC) was relatively small, which may limit the statistical power to some extent. For example, module segregation had

no significant correlations with NCT-A time and venous ammonia levels, which was inconsistent with our expectation. We suspect this result may be due to the modest sample size. Second, in order to ensure image quality and success rate of completing the examination, only 15 diffusion-encoding gradient directions and  $b$  value of 800 s/mm<sup>2</sup> were used in DTI acquisition as normal. However, more diffusion directions could be beneficial for detection of crossing fibers (41), while a high  $b$  value could improve the sensitivity of fraction anisotropy value changes in WM (42). Third, although the neuropsychological tests applied in our study are widely used in the clinic and recommended by expert consensus, more neuropsychological tests should be added in future studies to assess the abnormalities more accurately and comprehensively. These limitations offer clear directions for future studies, such as sample size enlargement, advanced image acquisition protocol, and longitudinal study for further investigation.

In conclusion, patients with MHE in our study manifested some specific brain structural connectome alterations. These changed patterns of topologic properties may underlie the abnormal cognitive performance in MHE patients and contribute to the neurophysiologic mechanisms involved. Moreover, our findings implied that the aberrant brain structural network may be used as a marker for monitoring MHE and predicting its prognosis.

#### Financial disclosure

This research was supported by grants from the Health Commission Foundation of Chongqing (Grant No.2017MSXM030 to Wei Zhang).

#### Acknowledgements

We gratefully thank all the staffs of Hepatology Treatment and Research Center of the Second Affiliated Hospital of Chongqing Medical University, Chongqing, China for their valuable help.

#### Conflict of interest disclosure

The authors declared no conflicts of interest.

#### References

- Xiao G, Ye Q, Han T, Yan J, Sun L, Wang F. Study of the sleep quality and psychological state of patients with hepatitis B liver cirrhosis. *Hepatology Res* 2018; 48:E275–E282. [CrossRef]
- Ampuero J, Montoliú C, Simón-Talero M, et al. Minimal hepatic encephalopathy identifies patients at risk of faster cirrhosis progression. *J Gastroenterol Hepatol* 2018; 33:718. [CrossRef]
- Urios A, Mangas-Losada A, Gimenez-Garzo C, et al. Altered postural control and stability in cirrhotic patients with minimal hepatic encephalopathy correlate with cognitive deficits. *Liver Int* 2017; 37:1013–1022. [CrossRef]

- Yildirim M. Falls in patients with liver cirrhosis. *Gastroenterol Nurs* 2017; 40:306–310. [CrossRef]
- Dhiman RK, Saraswat VA, Sharma BK, et al. Minimal hepatic encephalopathy: consensus statement of a working party of the Indian National Association for Study of the Liver. *J Gastroenterol Hepatol* 2010; 25:1029–1041. [CrossRef]
- David M, Sophie A, Alexa M, Ed B. Age-related changes in modular organization of human brain functional networks. *Neuroimage* 2009; 44:715–723. [CrossRef]
- Hsu TW, Wu CW, Cheng YF, et al. Impaired small-world network efficiency and dynamic functional distribution in patients with cirrhosis. *PLoS One* 2012; 7:e35266. [CrossRef]
- Deuker L, Bullmore ET, Smith M, et al. Reproducibility of graph metrics of human brain functional networks. *Neuroimage* 2009; 47:1460–1468. [CrossRef]
- Zhang LJ, Zheng G, Zhang L, et al. Disrupted small world networks in patients without overt hepatic encephalopathy: A resting state fMRI study. *Eur J Radiol* 2014. [CrossRef]
- Chen HJ, Chen QF, Liu J, Shi HB. Aberrant salience network and its functional coupling with default and executive networks in minimal hepatic encephalopathy: a resting-state fMRI study. *Sci Rep* 2016; 6:27092. [CrossRef]
- Chen HJ, Jiang LF, Sun T, Liu J, Chen QF, Shi HB. Resting-state functional connectivity abnormalities correlate with psychometric hepatic encephalopathy score in cirrhosis. *Eur J Radiol* 2015; 84:2287–2295. [CrossRef]
- Yang ZT, Chen HJ, Chen QF, Lin H. Disrupted brain intrinsic networks and executive dysfunction in cirrhotic patients without overt hepatic encephalopathy. *Front Neurol* 2018; 9:14. [CrossRef]
- Park HJ, Friston K. Structural and functional brain networks: from connections to cognition. *Science* 2013; 342:1238411. [CrossRef]
- Li X, Ma C, Sun X, et al. Disrupted white matter structure underlies cognitive deficit in hypertensive patients. *Eur J Radiol* 2016; 26:2899–2907. [CrossRef]
- Galantucci S, Agosta F, Stefanova E, et al. Structural brain connectome and cognitive impairment in parkinson disease. *Radiology* 2017; 283:515–525. [CrossRef]
- Chen HJ, Shi HB, Jiang LF, Li L, Chen R. Disrupted topological organization of brain structural network associated with prior overt hepatic encephalopathy in cirrhotic patients. *Eur Radiol* 2018; 28:85–95. [CrossRef]
- Ferenci P, Lockwood A, Mullen K, Tarter R, Weissenborn K, Blei AT. Hepatic encephalopathy—definition, nomenclature, diagnosis, and quantification: final report of the working party at the 11th World Congresses of Gastroenterology, Vienna, 1998. *Hepatology* 2002; 35:716–721. [CrossRef]
- Bao ZJ, Qiu DK, Ma X, et al. The application of psychometric measures in diagnosis of minimal hepatic encephalopathy. *Chin J Dig* 2006; 26:606–609.
- Gou L, Zhang W, Li C, et al. Structural brain network alteration and its correlation with structural impairments in patients with depression in de novo and drug-naïve Parkinson's disease. *Front Neurol* 2018; 9:608. [CrossRef]
- Rubinov M, Sporns O. Complex network measures of brain connectivity: uses and interpretations. *NeuroImage* 2010; 52:1059–1069. [CrossRef]

21. Mu J, Chen T, Liu Q, et al. Abnormal interaction between cognitive control network and affective network in patients with end-stage renal disease. *Brain Imaging Behav* 2018; 12:1099–1111. [\[CrossRef\]](#)
22. Zalesky A, Fornito A, Bullmore ET. Network-based statistic: identifying differences in brain networks. *Neuroimage* 2010; 53:1197–1207. [\[CrossRef\]](#)
23. Nigro S, Riccelli R, Passamonti L, et al. Characterizing structural neural networks in de novo Parkinson disease patients using diffusion tensor imaging. *Human Brain Mapp* 2016; 37:4500–4510. [\[CrossRef\]](#)
24. Bullmore ET, Bassett DS. Brain graphs: graphical models of the human brain connectome. *Annu Rev Clin Psychol* 2011; 7:113–140. [\[CrossRef\]](#)
25. Irimia A, Van Horn JD. The structural, connectomic and network covariance of the human brain. *Neuroimage* 2013; 66:489–499. [\[CrossRef\]](#)
26. Qin J, Liu H, Wei M, et al. Reconfiguration of hub-level community structure in depressions: A follow-up study via diffusion tensor imaging. *J Affect Disord* 2017; 207:305–312. [\[CrossRef\]](#)
27. Lin WC, Hsu TW, Chen CL, et al. Connectivity of default-mode network is associated with cerebral edema in hepatic encephalopathy. *PLoS One* 2012; 7:e36986. [\[CrossRef\]](#)
28. Nardone R, Taylor AC, Holler Y, Brigo F, Lochner P, Trinkka E. Minimal hepatic encephalopathy: A review. *Neurosci Res* 2016; 111:1–12. [\[CrossRef\]](#)
29. Munakata Y, Herd SA, Chatham CH, Depue BE, Banich MT, O'Reilly RC. A unified framework for inhibitory control. *Trends Cogn Sci* 2011; 15:453–459. [\[CrossRef\]](#)
30. Zeharia N, Hofstetter S, Flash T, Amedi A. A whole-body sensory-motor gradient is revealed in the medial wall of the parietal lobe. *J Neurosci* 2019; 39:7882–7892. [\[CrossRef\]](#)
31. Ilieva IP, Hook CJ, Farah MJ. Prescription stimulants' effects on healthy inhibitory control, working memory, and episodic memory: a meta-analysis. *J Cogn Neurosci* 2015; 27:1069–1089. [\[CrossRef\]](#)
32. Baum GL, Ciric R, Roalf DR, et al. Modular segregation of structural brain networks supports the development of executive function in youth. *Curr Biol* 2017; 27:1561–1572. [\[CrossRef\]](#)
33. Heuvel MP, Van Den, Kahn RS, Joaquín GI, Olaf S. High-cost, high-capacity backbone for global brain communication. *Proc Natl Acad Sci USA* 2012; 109:11372–11377. [\[CrossRef\]](#)
34. Crossley NA, Mechelli A, Vertes PE, et al. Cognitive relevance of the community structure of the human brain functional coactivation network. *Proc Natl Acad Sci USA* 2013; 110:11583–11588. [\[CrossRef\]](#)
35. Alexander-Bloch AF, Vertes PE, Stidd R, et al. The anatomical distance of functional connections predicts brain network topology in health and schizophrenia. *Cereb Cortex* 2013; 23:127–138. [\[CrossRef\]](#)
36. Griffa A, Baumann PS, Thiran JP, Hagmann P. Structural connectomics in brain diseases. *Neuroimage* 2013; 80:515–526. [\[CrossRef\]](#)
37. Crossley NA, Mechelli A, Scott J, et al. The hubs of the human connectome are generally implicated in the anatomy of brain disorders. *Brain* 2014; 137:2382–2395. [\[CrossRef\]](#)
38. Chen HJ, Chen QF, Yang ZT, Shi HB. Aberrant topological organization of the functional brain network associated with prior overt hepatic encephalopathy in cirrhotic patients. *Brain Imaging Behav* 2019; 13:771–780. [\[CrossRef\]](#)
39. Yu Y, Zhang B, Niu R, Li Y, Liu Y. The Relationship between biological motion-based visual consciousness and attention: an electroencephalograph study. *Neuroscience* 2019; 415:230–240. [\[CrossRef\]](#)
40. Weissenborn K. Hepatic encephalopathy: definition, clinical grading and diagnostic principles. *Drugs* 2019; 79:5–9. [\[CrossRef\]](#)
41. Vaessen MJ, Hofman PA, Tijssen HN, Aldenkamp AP, Jansen JF, Backes WH. The effect and reproducibility of different clinical DTI gradient sets on small world brain connectivity measures. *Neuroimage* 2010; 51:1106–1116. [\[CrossRef\]](#)
42. Hui ES, Cheung MM, Chan KC, Wu EX. B-value dependence of DTI quantitation and sensitivity in detecting neural tissue changes. *Neuroimage* 2010; 49:2366–2374. [\[CrossRef\]](#)